



Cite this article: Bedoya CL, Nelson XJ, Brockerhoff EG, Pawson S, Hayes M. 2022 Experimental characterization and automatic identification of stridulatory sounds inside wood. *R. Soc. Open Sci.* **9**: 220217. <https://doi.org/10.1098/rsos.220217>

Received: 6 March 2022

Accepted: 8 July 2022

Subject Category:

Physics and biophysics

Subject Areas:

acoustics/environmental science

Keywords:

acoustic communication, bark beetles, forest insects, Scolytinae, sound production

Author for correspondence:

Carol L. Bedoya

e-mail: clbedoya.contact@gmail.com

[†]Present address: Atarau Sanctuary, PO Box 2341, Christchurch, 8140, New Zealand.

[‡]Present address: School of Forestry, University of Canterbury, Private Bag 4800, Christchurch, New Zealand.

Electronic supplementary material is available online at <https://doi.org/10.6084/m9.figshare.c.6098720>.

Experimental characterization and automatic identification of stridulatory sounds inside wood

Carol L. Bedoya^{1,†}, Ximena J. Nelson¹, Eckehard G. Brockerhoff^{1,3,4}, Stephen Pawson^{4,‡} and Michael Hayes²

¹School of Biological Sciences, and ²Department of Electrical and Computer Engineering, University of Canterbury, Private Bag 4800, Christchurch, New Zealand

³Swiss Federal Research Institute WSL, Zürcherstrasse 111, 8903 Birmensdorf, Switzerland

⁴SCION (New Zealand Forest Research Institute), PO Box 29237, Christchurch, New Zealand

CLB, 0000-0002-7013-7083; XJN, 0000-0003-4301-2928; EGB, 0000-0002-5962-3208; SP, 0000-0003-2980-4873; MH, 0000-0002-6712-9509

The propagation of animal vocalizations in water and in air is a well-studied phenomenon, but sound produced by bark and wood-boring insects, which feed and reproduce inside trees, is poorly understood. Often being confined to the dark and chemically saturated habitat of wood, many bark- and woodborers have developed stridulatory mechanisms to communicate acoustically. Despite their ecological and economic importance and the unusual medium used for acoustic communication, very little is known about sound production in these insects, or their acoustic interactions inside trees. Here, we use bark beetles (Scolytinae) as a model system to study the effects of wooden tissue on the propagation of insect stridulations and propose algorithms for their automatic identification. We characterize distance dependence of the spectral parameters of stridulatory sounds, propose data-based models for the power decay of the stridulations in both outer and inner bark, provide optimal spectral ranges for stridulation detectability and develop automatic methods for their detection and identification. We also discuss the acoustic discernibility of species cohabitating the same log. The species tested can be acoustically identified with 99% of accuracy at distances up to 20 cm and detected to the greatest extent in the 2–6 kHz frequency band. Phloem was a better medium for sound transmission than bark.

1. Background

Forest soundscapes are a recurrent topic in acoustic, ecological and sociological studies [1–3]. These sounds can inform our understanding of the interactions between animals and their habitat [1,4]. Nonetheless, research effort is biased toward sounds that propagate through air or water—neglecting local soundscapes occurring in other propagation media. One of these is wood, within which some insects (e.g. bark beetles (Scolytinae), wood borers (e.g. Cerambycidae, Bostrichidae and Ptinidae), pinhole borers (Platypodinae) and termites (Isoptera)) communicate acoustically [5–7]. We know very little about communicatory interactions inside wood/bark and the transmission of acoustic information within these media [8]. In order to address this, we use bark beetles (Coleoptera: Curculionidae: Scolytinae) to study the propagation and attenuation of stridulatory sounds inside trees. We also propose strategies for the automatic acoustic detection and identification of bark beetles and woodborers so that they can be studied without disrupting their natural habitat.

Bark beetles are a subfamily of weevils that spend most of their life cycle inside plant tissue [9,10] and are one of the very few animals that have evolved sound production mechanisms to communicate inside plants [7,11]. Although ‘bark beetle’ is usually used to refer to all the Scolytinae, ‘true bark beetles’ are the subset that live, feed and reproduce in the phloem tissue of trees (i.e. phloeophagy) [12,13]. There are *ca* 6000 described species of Scolytinae [9] distributed in all regions of the world, except Antarctica [10]. Previous studies of bark beetle life history and behaviour typically focus on less than 1% of species that are important forest pests that attack and potentially kill trees [9,14].

Bark beetles typically construct an intricate system of tunnels (also referred to as galleries) within trees, where adults and larvae feed and complete their development [11]. Some bark beetles use airborne pheromones to communicate over large distances that facilitate aggregation or disrupt aggregations of conspecifics [10], and acoustic signals, on and within the host, for intraspecific communication over short distances [15,16]. However, the sounds of only a few, typically economically important, species have been reported in the literature. From the limited data available, acoustic signalling appears to be widespread within the group, but remains poorly documented [7,17,18]. Sound production in Scolytinae is mediated by three predominant types of stridulatory organs: elytra-tergal, vertex-pronotal and gula-prosternal [7,17,18]. These organs can arise in one, both or neither of the sexes, and, in studies to date where both sexes stridulate, both the organ and the signals are usually sexually dimorphic [7,11,18]. Each stridulatory organ consists of two parts: (i) a static file of teeth, also known as *pars stridens* and (ii) a movable plectrum consisting of a set of spines, tubercles or teeth that rubs against the static file [17]. Acoustic characteristics of the stridulatory sounds vary between species [19–21]. Such characteristics are also dependent on the behavioural context [19,21], as acoustic communication is used in several functions, including distress, pre-mating recognition, rivalry and copulation [17–19].

Given how little we know about bark beetle and woodborer stridulatory behaviour in general, it is unsurprising that the effect of the propagation medium on their sounds has not been assessed. Previous studies have mostly focused on the analysis of mechanical sounds (e.g. chewing), or the vibrational movement of insect larvae and pupae [22–25]. However, the specific effect of wood and bark tissue on the propagation of acoustic communication (i.e. signals produced by acoustic organs) has yet to be investigated. Several theoretical methods have been developed for studying sound attenuation and absorption by trees [26–28] and wood [29,30]; however, these models are typically used to estimate wood properties from bulk wave propagation.

The goal of our study was to address several unresolved issues related to the propagation of stridulatory sounds inside wood, so that this new information can be used for the acoustic detection and identification of insects inside trees. We analysed the acoustic signals of two bark beetles, *Hylastes ater* Paykull and *Hylurgus ligniperda* (Fabricius), in order to characterize distance-dependent changes in the spectro-temporal features of stridulations propagating through wood. We determine which part of the audible spectrum is the most suitable to acoustically detect stridulations and investigate the maximum distances at which the presence of a bark beetle can be acoustically detected and the species identified. Then, we propose a data-based model for the attenuation of stridulatory sounds through wood, taking into consideration the type of tissue and its width. Finally, we implement a method for the acoustic detection and identification of stridulations, and provide suggestions for future improvements.

2. Methods

2.1. Subjects

Hylastes ater and *H. ligniperda* were selected to study the propagation of stridulatory sounds inside wood because physical interactions (e.g. touching) trigger stridulatory behaviour in males [7], and thus, sound



Figure 1. Size comparison of males of *Hylastes ater* (left) and *Hylurgus ligniperda* (right) on an American penny.

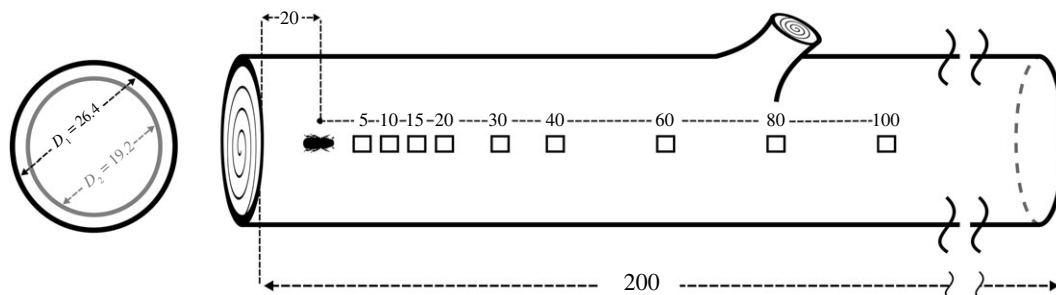


Figure 2. Experimental set-up for the analysis of sound propagation of two bark beetle species (*H. ligniperda* and *H. ater*) in wood. D_1 and D_2 are the average diameters of the *Pinus radiata* logs used for testing. A beetle was placed 20 cm from one end of the log. Stridulatory sounds produced by the individual were recorded at nonlinearly spaced distances from 5 to 100 cm. This procedure was repeated in the bark and phloem layer of each log. Dimensions in cm (not to scale).

production can be manually elicited by the researcher. *H. ligniperda* has one of the highest known calling rates of all bark beetles [7,21] and tends to sing uninterruptedly for long periods (i.e. tens of minutes). *H. ater* also responds acoustically to physical stimulation, although the duration of the stridulatory behaviour is shorter than in *H. ligniperda*. Both species are less than 6 mm in body length (*H. ater* 4.0 mm and *H. ligniperda* 5.0 mm, on average; figure 1) and colonize a variety of conifers, but mainly *Pinus* spp., including economically important species [31]. Insects were manually collected from recently felled *Pinus radiata* D. Don logs in Bottle Lake Forest, Christchurch, New Zealand ($-43^{\circ}27'8.64''$ S, $172^{\circ}41'42.00''$ E).

2.2. Experimental set-up

Recordings were acquired using a 352A24 monoaxial accelerometer (PCB piezotronics, Depew, USA) and a 744 T recorder (Sound Devices, Reedsburg, USA). Analysed signals were of 1 min duration at a sampling frequency of 44100 Hz, 48 dB gain and 24-bit resolution. Two *P. radiata* logs (200 cm long, with respective mean \pm s.d. diameters of 19.2 ± 0.3 and 26.4 ± 0.7 cm) were used during the experiment. The logs were held inside a temperature-controlled room at a constant temperature of 23°C for the duration of the experiments (14 days). Humidity inside the phloem was measured using a SHT85 sensor (Sensirion, Stäfa, Switzerland) after collecting data from each individual in each log in order to ensure humidity did not decline substantially.

2.3. Data collection

To estimate the effect of the outermost bark layer on signal acquisition, the experimental procedure was performed on the bark surface and inside the phloem tissue of two *P. radiata* logs of different diameters. Most bark- and woodborers live underneath the outermost bark tissue; thus, whether to pierce the bark is an important question that naturally arises before performing acoustic data acquisition in trees. Therefore, we tested tissue effects on each log, which had different average thicknesses of bark (3.3 ± 1.2 mm; 8.5 ± 1.3 mm) and phloem (2.6 ± 0.5 mm; 3.1 ± 0.8 mm). Subsequently, we recorded acoustic signals of *H. ligniperda* and *H. ater* at nine pre-allocated distances (5, 10, 15, 20, 30, 40, 60, 80 and 100 cm) from the position of the stridulating beetle (figure 2). Five beetles of each species were individually recorded in both logs with sensors located on the bark and in the phloem tissue at the

respective nine distances ($n = 5$ per species, nine distances, three factors (beetle species, tissue type, log thickness), two levels per factor, $n = 45$ per treatment, 360 recordings in total).

Beetles were individually inserted into a pre-drilled hole (5 mm diameter) through the outer bark into the phloem, at a distance of 20 cm from the edge of the log (figure 2). Then, the elytra of each beetle was softly touched with a paintbrush (Bockingford, 5700R, size 1) to trigger sound production as per Bedoya *et al.* [7,21]. To record stridulations, the vibrational sensor (accelerometer) was attached to the bark, along the grain, using Blu-Tack™ at any of the nine discrete distances from 5 to 100 cm (figure 2). Once the signal was acquired, the sensor was randomly moved to a different position and data collection started again until data were acquired from all nine pre-allocated distances for each beetle. After signals were recorded on the bark of each of the two logs, 1 cm² holes were carved into the bark until the phloem tissue was accessible. Then, the sensor was placed on the phloem and the experimental procedure was repeated, as previously described on the bark, using the same individuals.

2.4. Data analysis

2.4.1. Spectrogram and power spectrum estimation

Spectrograms used for visualization were generated using a FFT of 1024 bins and a symmetric flat top window of 1024 samples with 3/4 overlap. Plots of power spectral density (PSD) were generated by averaging the PSDs of all test subjects for each species at each of the analysed distances. The frequency-dependent power decay was estimated by averaging the mean PSD values from the signals of each species at every pre-determined distance (5–100 cm) in frequency bands of 2 kHz. Power spectral densities were estimated using Welch's method. Power values hereafter are shown in dB full scale (dBFS), using the maximum power value of all signals as a reference for the scaling.

2.4.2. Experimental models

Attenuation models were generated by fitting the average power decay from individuals of *H. ligniperda* and *H. ater* to exponential functions ($P(z) = \psi e^{-\alpha z} - c$), where α is the frequency-dependent attenuation coefficient and z is the distance between the sensor and the source. ψ and c are model constants in dB, where c depends on the noise level ($N = 10^{-c}$). The exponential fitting was performed using nonlinear least squares on the averaged power levels at each distance. Recordings were separated by species, type of tissue and tissue width, and were modelled independently. The relationship between the tissue width and the attenuation coefficient was determined *a posteriori* by fitting a linear model between the values of both parameters. The root mean square error was estimated as a measure of goodness of fit, and 95% confidence intervals were shown for the estimated parameters.

2.4.3. Automatic acoustic detection and identification

Since acoustic features are dependent on distance from the source, we implemented several supervised and unsupervised automatic acoustic detection methods to determine the maximum distance at which species can be reliably identified. We extracted all the stridulations from our recordings using an energy-based segmenter and estimated five acoustic features for each of them (centroid frequency, dominant frequency, bandwidth, duration and mean amplitude). Then, we used four different clustering algorithms and seven classification techniques to estimate the accuracy of the species identification.

2.4.3.1. Segmentation and feature extraction

Stridulations were segmented from the spectrogram using a threshold-based approach [21]. The method consisted of averaging the values of the spectrogram in the time domain, and using the mean value of this new vector as a threshold for identifying the start and end of a stridulation. Five acoustic features were then estimated for each stridulation: the centroid frequency, dominant frequency, bandwidth, duration and amplitude. The centroid frequency f_c was estimated using: $f_c = \sum_{i=1}^{N_t} f_i u_i / \sum_{i=1}^{N_t} u_i$, where u_i is the i th value of the mean spectrum and f_i is the current frequency bin. This frequency is analogous to the centre of mass in mechanical systems [32]. The dominant frequency was the frequency bin with the maximum power value. Bandwidths were determined by the upper and lower cut-off frequencies of the mean spectrum of each call (cut-off 3 dB). Duration was defined as the length of the call. The mean power of the spectrum was used as the amplitude feature. All the acoustic features were normalized (0–1) before being used as input for the clustering and classification algorithms. Since acoustically detecting the presence of bark

beetles is possible even if the specific species cannot be discerned, we also estimated average centroid frequencies throughout the log in order to find the distance at which species are spectrally distinguishable.

2.4.3.2. Clustering and classification

To evaluate the discernibility of species with distance, all stridulations were clustered into two groups using four unsupervised learning techniques (K-means, Fuzzy c-means (FCM), DBSCAN and Gaussian mixture models (GMM)) applied to the five extracted acoustic features. Comparisons were made against the call duration in order to show how a combination of spectro-temporal features increases species identification with distance. For the K-means, the squared Euclidean distance was used as the metric for minimization. For the FCM, the fuzzy partition matrix exponent that controls the degree of fuzzy overlap (i.e. the fuzzifier) was set to 2. In the GMM case, model likelihood was optimized using the expectation-maximization algorithm. Finally, for DBSCAN, 50 was selected as the minimum number of points and $\epsilon = 0.25$.

All the classification algorithms (i.e. supervised learning) were trained to identify both species using fivefold cross-validation (80% training – 20% test) at each specific distance. The decision tree used the Gini's diversity index as split criterion with four as the maximum number of splits. Linear and quadratic discriminant analyses used full covariance matrices. The Naive Bayes Classifier was implemented with a Gaussian kernel, while support vector machines (SVMs) were tested with linear, quadratic, cubic and Gaussian kernels. Results for the K-nearest neighbours algorithm (KNN) are presented for Euclidean, cosine and Minkowski distances using equal distance weights and 10 neighbours. Decision trees, linear discriminant (LD) analyses and KNNs were also used in ensemble. Bag ensemble was used for the decision tree (number of learners = 30, maximum number of splits = 712), whereas both LD and KNN used subspace ensemble (30 learners and 3 subspace dimensions).

Accuracies, defined as $(Tp + Tn)/(Tp + Tn + Fp + Fn)$, were reported as general performance measurements for all classification and clustering algorithms. Here, Tp , Tn , Fp and Fn are the rates of true positives, true negatives, false positives and false negatives, respectively. Bark beetle acoustic terminology is based on Bedoya *et al.* [21]. All figures and mathematical models were coded in Matlab 2018b.

3. Results

Hylurgus ligniperda and *H. ater* possess single-note quasiperiodically repeating calls that were strongly attenuated by the phloem (figure 3). With increasing distance, signal intensity decreased and spectral content (e.g. bandwidth) compressed, while some temporal features (e.g. duration) shrank, and others (e.g. inter-syllable interval) expanded due to frequency-dependent attenuation [33] (figure 3).

3.1. Power decay

We estimated the power spectra of recordings with *H. ligniperda* and *H. ater* stridulations (figure 4). In both species, power was mostly concentrated between 3 and 7 kHz, and decayed with distance. *H. ligniperda*, the bigger species, had very noticeable power distributions up to 40 cm, whereas *H. ater* had a pronounced decrease in power after 20 cm (figure 4).

In order to localize a specific frequency band for acoustic detection, we divided the spectrum into 2 kHz bands and measured the average power decay at each distance (figure 5). The most suitable frequency range for detecting individuals at long distances was 4–6 kHz (figures 3 and 5). Power decayed significantly after 20 cm for *H. ater* and 40 cm for *H. ligniperda* (figure 3). After 40 cm, sounds were slightly perceptible for some *H. ligniperda* individuals, but only in the 2–6 kHz frequency band (figures 3 and 5).

3.2. Attenuation modelling

Our experimental results showed that tissue width significantly reduced power over distance—the wider the tissue (bark/phloem), the more the signal amplitude was attenuated (figure 6). Attenuation in bark was stronger than in phloem, and stridulations of *H. ater* (the smaller species) attenuated faster than those of *H. ligniperda* (figure 6 and table 1). The phloem is the tissue that transports the soluble organic compounds inside trees; thus, it is more humid and presents less impedance to sound transmission [34].

Aside from the exponential models, we generated linear models to correlate our attenuation coefficients (α) with the width of the tissue:

$$\alpha_{\text{bark}} = -0.191 \cdot w_{\text{bark}} + 0.275 \quad (3.1)$$

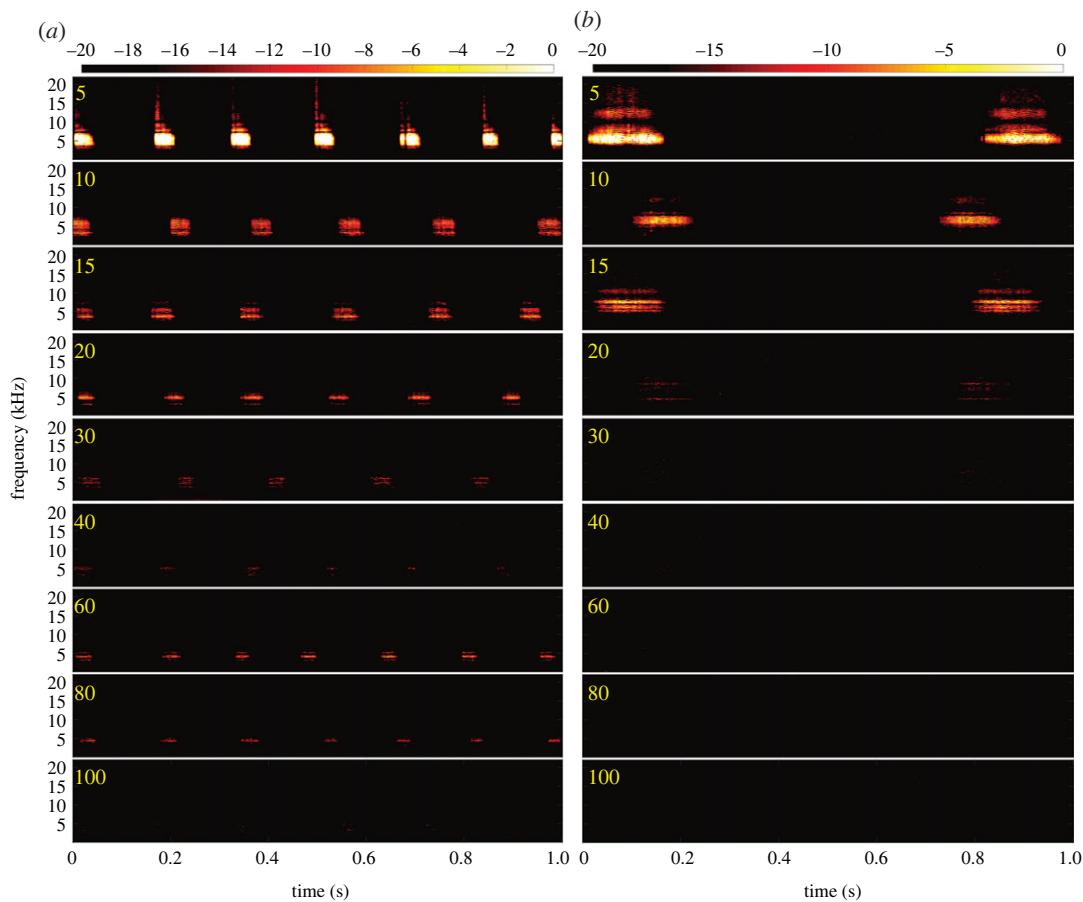


Figure 3. Stridulations of two individuals of *H. ligniperda* (a) and *H. ater* (b) on *Pinus radiata* phloem recorded from 5 (top) to 100 (bottom) cm from source. Colourbars in dBFS. In some individuals, sounds of *H. ligniperda* were detectable at 100 cm, while those of the smaller *H. ater* were only detectable up to 40 cm. A normalized version of these spectrograms is shown in the electronic supplementary material, figure S1.

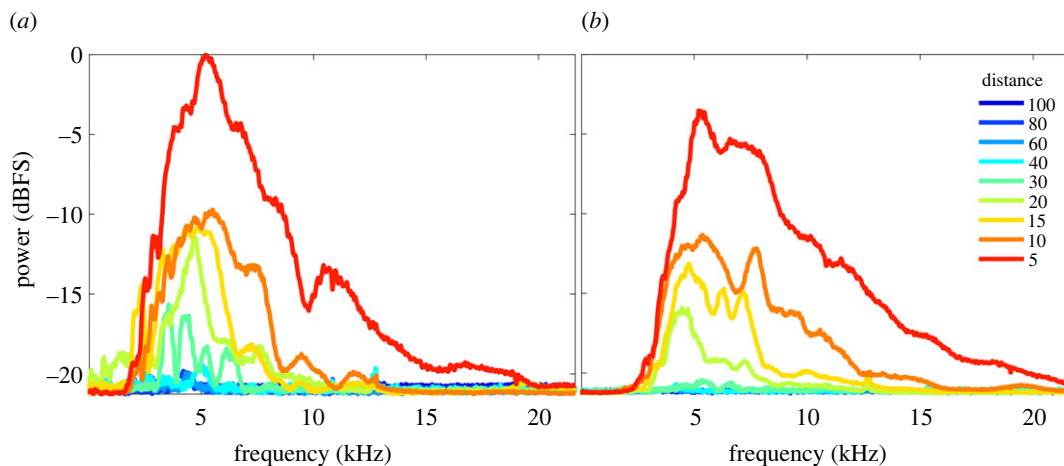


Figure 4. Average PSD of the stridulatory sounds of (a) *H. ligniperda* and (b) *H. ater* recorded at distances of 5–100 cm from source. Most power was concentrated between 3 and 7 kHz. Averaging was for all individuals of each species, after PSD estimation for the entire dataset (phloem and bark). A normalized version of these spectra is shown in the electronic supplementary material, figure S2.

and

$$\alpha_{\text{phloem}} = -2.030 \cdot w_{\text{phloem}} + 0.724, \quad (3.2)$$

where α_{bark} and α_{phloem} are the attenuation coefficients (dB cm⁻¹) for bark and phloem, depending on the width of the bark (w_{bark}) and the phloem (w_{phloem}), respectively, with widths in cm.

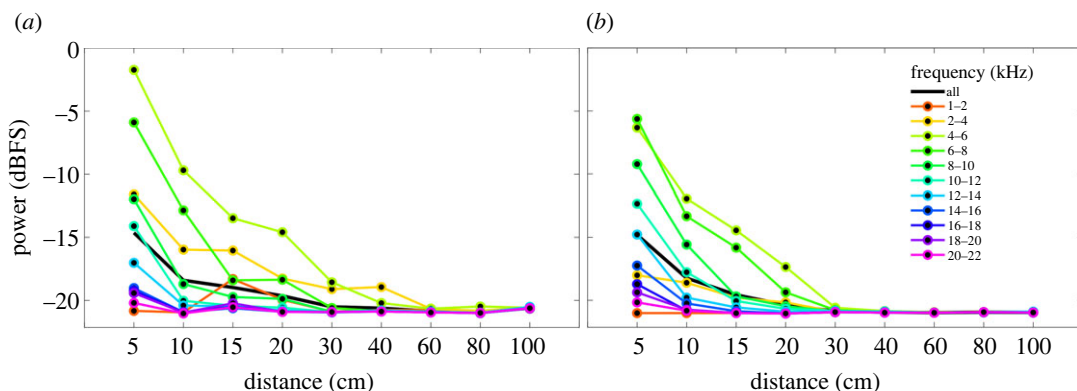


Figure 5. Average power decay with distance of the stridulations of (a) *H. ligniperda* and (b) *H. ater* estimated in frequency bands of 2 kHz for the entire dataset (phloem and bark). Most stridulations could be detected at their furthest reach using solely the 4–6 kHz frequency band, where spectral components were less attenuated. A version of these plots with error bars is shown in the electronic supplementary material, figure S3.

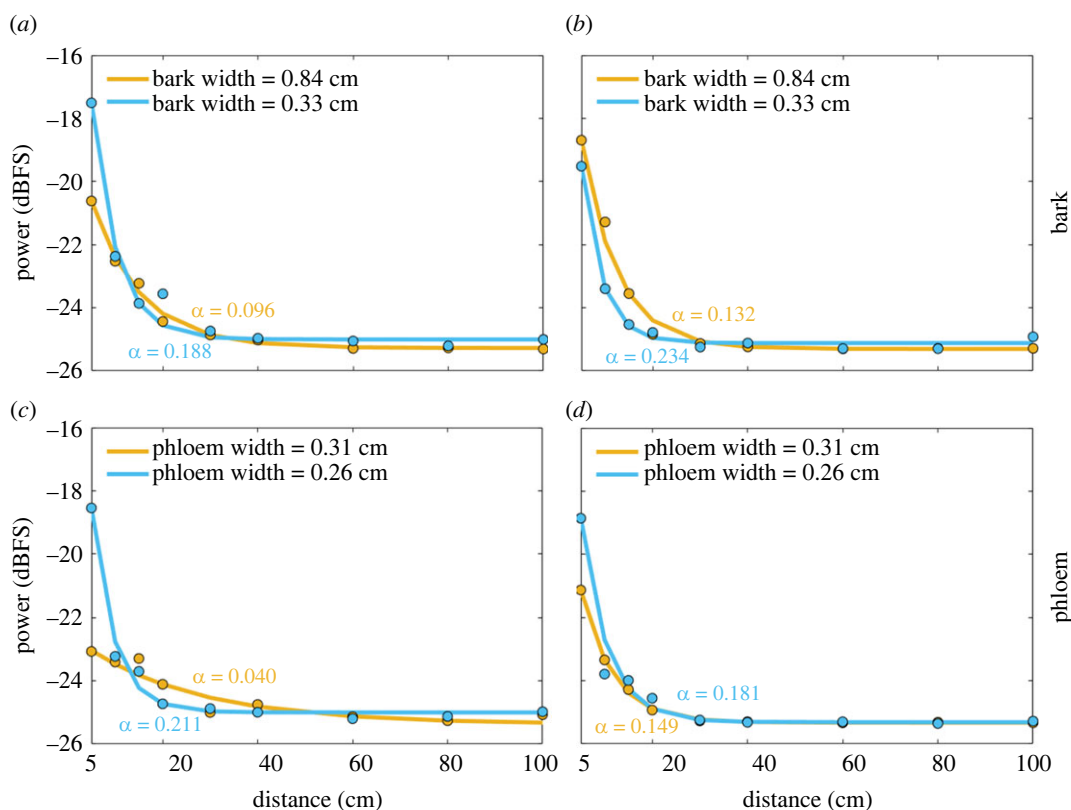


Figure 6. Experimental models for the power attenuation with distance of stridulatory sounds inside *Pinus radiata* logs. α is the attenuation coefficient of an exponentially decaying function ($\psi e^{(-\alpha z)} - c$). Models are shown for two different types of tissue (phloem and bark) of different widths, and two bark beetle species (*H. ligniperda* (a,c) and *H. ater* (b,d)). Data points represent the average power for all the individuals at that distance.

3.3. Species identification

Our data showed that, for *H. ater*, the centroid frequency stabilized at 30 cm, and that beyond 40 cm, the two species were indistinguishable using solely spectral content (figure 7). Analogously, in the temporal domain, both species could not be discriminated using solely call duration at distances beyond 20 cm (electronic supplementary material, figure S4).

At distances up to 20 cm, all algorithms were able to accurately and automatically (greater than 97%) discriminate stridulations of *H. ligniperda* from *H. ater* (table 2). After 40 cm, automatic identification reached chance levels, since the stridulations were so attenuated that they could not be discerned

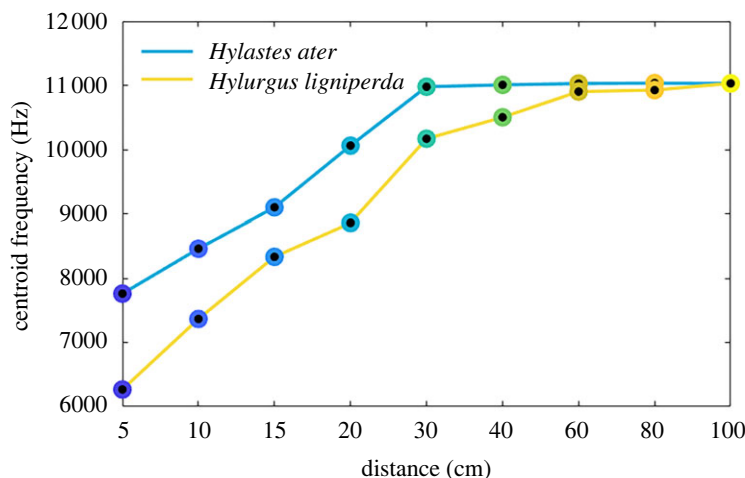


Figure 7. Centroid frequency of *H. ligniperda* and *H. ater* stridulations. Data points are averages from all five individuals. Beyond 40 cm species-specific stridulations become spectrally indistinguishable.

Table 1. Parameters of the experimental models for the power decay with distance of stridulatory sounds inside *Pinus radiata* bark and phloem. Power levels at each distance were fitted to an exponentially decaying function $P(z) = \psi e^{(-\alpha z)} - c$, where z is the distance in cm and α is the attenuation coefficient. The RMSE is shown as a measure of goodness of fit.

species	tissue	width (cm)	α	ψ	c	RMSE
<i>H. ligniperda</i>	bark	0.84	0.096	7.560	25.274	0.1677
<i>H. ligniperda</i>	bark	0.33	0.188	19.191	25.002	0.4414
<i>H. ligniperda</i>	phloem	0.31	0.040	2.860	25.369	0.2096
<i>H. ligniperda</i>	phloem	0.26	0.211	18.604	24.998	0.3035
<i>H. ater</i>	bark	0.84	0.132	12.838	25.304	0.2063
<i>H. ater</i>	bark	0.33	0.234	18.139	25.118	0.1599
<i>H. ater</i>	phloem	0.31	0.149	8.866	25.330	0.0347
<i>H. ater</i>	phloem	0.26	0.181	15.976	25.313	0.2771

(table 2). This phenomenon can be visualized by plotting an ordination of amplitude, frequency and time features in two-dimensional space, where compact and segregated clusters are observable up to 20 cm for both species (figure 8). After 20 cm, the clusters became sparser until gradually merging at 60 cm, where stridulations of both species are embedded in the same subspace and cannot be discerned (figure 8).

4. Discussion

We characterized the propagation of stridulatory sounds of two bark beetle species (*H. ater* and *H. ligniperda*) through *P. radiata* logs, showing the effects of phloem and bark on signal attenuation over distance. We were able to correctly identify stridulatory sounds from insects of less than 6 mm length at distances of up to 40 cm. However, spectral content and signal amplitude attenuated with distance, particularly in the bark tissue. Beyond 20 cm from the beetle, distance effects reduce the beetle signal bandwidth, which removes the part of the spectrum that allows species identification, making *H. ligniperda* and *H. ater* stridulations difficult to distinguish. Nevertheless, the remaining content is sufficient to determine the presence of bark beetle activity beyond 40 cm, and additional temporal features may be used to tell species apart (e.g. call rate and inter-call interval), as these can be reliable species-specific descriptors [7].

In both species, power was concentrated between 3 and 7 kHz, which appears to be a general characteristic of the Scolytinae (see electronic supplementary material of [7]). We found that 4–6 kHz, where most of the energy is concentrated, was the optimal frequency band to detect stridulations.

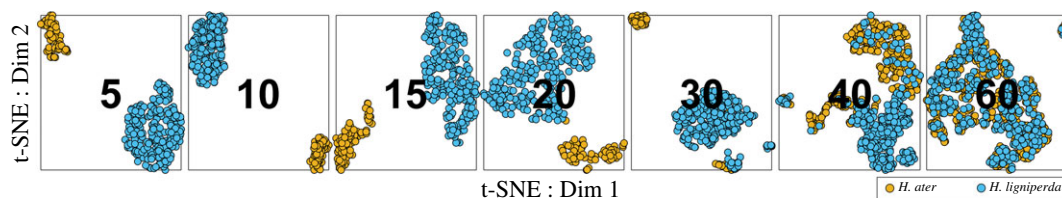


Figure 8. Two-dimensional t-SNE visualization of individual stridulations of *H. ligniperda* (blue) and *H. ater* (yellow) recorded at pre-determined distances (cm). Five acoustic features (mean amplitude, dominant frequency, centroid frequency, bandwidth and duration) were used for the ordination. Stridulations of both species become acoustically undistinguishable at 60 cm.

Table 2. Accuracy results for several supervised and unsupervised machine learning approaches tested for a bi-class clustering/classification task: discriminating *H. ligniperda* and *H. ater* stridulations at different distances.

algorithm	accuracy (%)						
	5 cm	10 cm	15 cm	20 cm	30 cm	40 cm	60 cm
Unsupervised learning							
K-means	100.0	100.0	99.7	99.3	90.6	74.5	51.9
FCM	99.6	100.0	100.0	99.0	81.8	71.4	50.2
GMM	99.3	100.0	100.0	99.7	89.3	80.8	51.3
DBSCAN	100.0	98.0	99.7	99.7	91.8	71.6	51.6
Supervised learning							
decision tree	100.0	99.2	100.0	98.4	95.0	84.9	50.5
LD	100.0	100.0	99.7	99.7	91.2	80.5	52.3
quadratic discriminant	99.6	100.0	100.0	99.7	95.3	80.9	49.8
logistic regression	100.0	100.0	100.0	99.3	91.2	81.4	52.6
Naive Bayes	100.0	99.6	99.7	99.0	90.9	85.8	52.3
SVM (linear)	100.0	100.0	99.3	99.7	92.1	81.9	51.3
SVM (quadratic)	100.0	100.0	99.3	99.3	95.6	86.2	48.2
SVM (cubic)	100.0	100.0	99.3	99.7	95.3	86.9	48.5
SVM (Gaussian)	100.0	100.0	99.7	99.7	97.2	87.2	46.7
KNN (Euclidean)	100.0	100.0	99.3	99.7	95.6	85.5	52.2
KNN (Cosine)	100.0	100.0	99.3	97.4	97.2	86.9	49.9
KNN (Minkowski)	100.0	100.0	99.3	99.0	96.5	87.1	48.0
bag ensemble (decision tree)	100.0	100.0	99.7	98.4	96.9	86.9	49.6
subspace ensemble (LD)	100.0	100.0	99.7	99.0	91.2	81.0	50.9
subspace ensemble (KNN)	100.0	100.0	100.0	99.3	97.2	88.1	50.1

This frequency is also one of the least attenuated by pine trees [27]. Our results concord with previous experimental models for the propagation of sound inside wood [26,27], suggesting an acoustic impedance matching between the beetle stridulatory mechanism and the medium. Measurements of sound speed in *Pinus radiata* have been previously reported for logs and standing trees from New Zealand forests [35]; consequently, these measurements were not part of our experimental design. The mean sound speed in *P. radiata* is $2277 \pm 496.1 \text{ m s}^{-1}$ (mean \pm s.d.) for standing trees and $2120 \pm 363.5 \text{ m s}^{-1}$ for 3.66 m long logs [35]. Accurate descriptions of the dependence of sound speed in *P. radiata* on tree age, type of tissue, length and width of the tree, and moisture content are described in Grabianowski *et al.* [36], Wang *et al.* [35] and Toulmin *et al.* [37].

We also propose a series of exponential models for the power decay of the stridulations depending on beetle species, type of tissue and distance. Removing the bark did not significantly reduce the signal

power, suggesting that beetles can be accurately detected without removing the bark. Furthermore, our machine learning analyses suggest that species can be reliably identified (greater than 97% accuracy) at short distances of less than 20 cm, and with relatively good accuracy (greater than 70%) up to 40 cm. After 40 cm, our experimental model shows that most of the energy has already dissipated, and none of the tested clustering or classification algorithms was able to provide accurate identification results. Nonetheless, the presence of bark beetles can still be detected at further distances in the 4–6 kHz frequency band if the species is large enough (e.g. *H. ligniperda*). The accuracies obtained using supervised and unsupervised approaches are almost identical up to 20 cm; from 30 cm onwards supervised learning techniques become advantageous. However, the increase in accuracy is not large enough to overcome the benefits of unsupervised learning (e.g. no need for data labelling). Also, the use of machine learning techniques on multiple spectro-temporal features significantly improves (greater than 40%) the species identification accuracy at distances above 20 cm when compared with a discrimination using solely call duration, doubling the distance at which a beetle can be accurately identified.

As bark beetles are among the smallest of the woodborers [9], for bigger taxa, such as some pinhole borers (Platypodinae), which tend to generate louder stridulations than most bark beetles [7], we would expect similar attenuation patterns and longer detectability ranges than those found here. The smallest known woodborer with acoustic communication capabilities (*Ips avulsus*, 2.5 mm) is relatively loud for its size and has a similar amplitude range to *H. ater* [7]. Consequently, we hypothesise that deploying an array of sensors spaced at distances of 40 cm should be enough to detect stridulations of any bark- or wood-boring species in logs similar to those of *P. radiata*. The key remaining issue for the detection of the potential presence of such insects is how to elicit *ad libitum* sound production under the bark of trees, so that the stridulations can be detected in a species-specific manner to identify the presence of woodborers in logs and standing trees. Chemical, acoustic and luminous stimuli can elicit acoustic communication in several species [11,38,39]. However, integrating these stimuli with acoustic detection and identification methods has yet to be addressed, especially when the target organism is hidden under the bark.

For acoustic identification purposes, deploying an array of sensors 20 cm apart is enough to detect and identify a species. At distances below 20 cm, between the source and the sensor, the spectral content of the stridulation does not change enough to make the species indistinguishable. Increasing the distance between sensors may increase the detectability range, but may affect the accuracy of the species identification. Depending on the application and the need for accuracy, 40 cm is a good compromise, as most stridulations are still detectable and the identification accuracy is above 70%. If the acoustic identification set-up is located in an environment with much background noise and the frequency range needs to be restricted, 4 to 6 kHz is a useful band to analyse, as this is where most of the energy is concentrated. Bark beetles live in the phloem, but part of their bodies are usually in contact with the bark tissue, generating a direct coupling with the drier outermost bark layer. Consequently, from an attenuation standpoint, piercing the tree in order to place the sensor in the phloem layer does not appear to provide a substantial benefit, as stridulations attain similar detectability ranges in both types of tissue. Bark is the most accessible contact point between the sensor and the tree stem; thus, placing the sensor on the bark surface of a tree or stem does not jeopardize species detection and does not produce tissue damage.

No studies have been performed on tree soundscapes or acoustic interactions of bark- or wood-boring beetles in their natural habitat, despite the prevalence of acoustic activity in insects living inside trees. Future work should focus on determining how a noisy field setting may affect the automatic identification accuracy of our approach, as this was tested in a controlled (i.e. noise-reduced) environment. In spite of this, our study provides a better understanding of the propagation of stridulations under the bark of trees and contributes towards the development of techniques to study bark- and woodborers in nature. We provide information on how these beetles may be acoustically detected and identified, where to position sensors, and in which part of the frequency of the acoustic spectrum to search for identifying information. We hope this study promotes understanding of acoustic communication inside tree tissues and its role in animal interactions. An appreciation of how stridulatory signals propagate inside tree tissues should aid in our understanding of colonization patterns, gallery structure and niche-partitioning between cohabitating species. We also hope this work establishes new ground for technological development to aid in automatic acoustic detection approaches for biosecurity purposes. As some bark beetles are of significant economic and biosecurity importance [14,40], a clear understanding of acoustic signal propagation through bark and wood can enhance efforts to determine the presence and species identity of potential pest species at borders.

Data accessibility. Acoustic datasets and algorithms used during this research are available at: Data: <https://doi.org/10.6084/m9.figshare.19233087.v2>. Code: <https://doi.org/10.5281/zenodo.6757369> [41].

Electronic supplementary material is available online at [42].

Authors' contributions. C.L.B.: conceptualization, data curation, formal analysis, investigation, methodology, software, validation, visualization, writing—original draft and writing—review and editing; X.J.N.: conceptualization, investigation, project administration, resources, supervision and writing—review and editing; E.G.B.: conceptualization, funding acquisition, investigation, project administration, resources, supervision and writing—review and editing; S.P.: conceptualization, resources and writing—review and editing; M.H.: conceptualization, formal analysis, methodology, supervision, validation, visualization, writing—original draft and writing—review and editing.

All authors gave final approval for publication and agreed to be held accountable for the work performed therein. Conflict of interest declaration. We declare we have no competing interests.

Funding. This project was supported by the New Zealand Ministry of Business, Innovation, and Employment (MBIE), grant no. C04X1407, the Better Border Biosecurity Collaboration (b3nz.org) via MBIE Core Funding to Scion and Catalyst: Seeding funding from the Royal Society of New Zealand (grant no. CSG-FRI1701).

Acknowledgements. This project was supported by the New Zealand Ministry of Business, Innovation, and Employment (MBIE), grant no. C04X1407, the Better Border Biosecurity Collaboration (b3nz.org) via MBIE Core Funding to Scion, and Catalyst: Seeding funding from the Royal Society of New Zealand (grant no. CSG-FRI1701).

References

- Dumyahn SL, Pijanowski BC. 2011 Soundscape conservation. *Landscape Ecol.* **26**, 1327–1344. (doi:10.1007/s10980-011-9635-x)
- Ross M, Masson GJ. 2017 The effects of preferred natural stimuli on humans' affective states, physiological stress and mental health, and the potential implications for well-being in captive animals. *Neurosci. Biobehav. Rev.* **83**, 46–62. (doi:10.1016/j.neubiorev.2017.09.012)
- Burivalova Z, Game ET, Butler RA. 2019 The sound of a tropical forest. *Science* **363**, 28–29. (doi:10.1126/science.aav1902)
- Pijanowski BC, Villanueva-Rivera LJ, Dumyahn SL, Farina A, Krause BL, Napolitano BM, Gage SH, Pieretti N. 2011 Soundscape ecology: the science of sound in the landscape. *BioScience* **61**, 203–216. (doi:10.1525/bio.2011.61.3.6)
- Birch MC, Keenleyside JJ. 1991 Tapping behavior is a rhythmic communication in the death-watch beetle, *Xestobium rufovillosum* (Coleoptera: Anobiidae). *J. Insect Behav.* **4**, 257–263. (doi:10.1007/BF01054618)
- Lai JCS, Oberst S, Evans TA. 2017 Termites thrive by using vibrations. In *24th Int. Congress on Sound and Vibration - ICSV 2017 USA* (ed. B Gibbs), London, UK, 23–27 July 2017, pp. 1–8. Auburn, AL: International Institute of Acoustics and Vibration.
- Bedoya CL, Hofstetter RW, Nelson XJ, Hayes M, Miller DR, Brockerhoff EG. 2021 Sound production in bark and ambrosia beetles. *Bioacoustics* **30**, 58–73. (doi:10.1080/09524622.2019.1686424)
- Hill *et al.*. 2019 *Biotremology: Studying Vibrational Behavior*. Cham, Switzerland: Springer.
- Kirkendall LR, Biedermann PH, Jordal BH. 2015 Evolution and diversity of bark and ambrosia beetles. In *Bark beetles: biology and ecology of native and invasive species* (eds F Vega, RW Hofstetter), pp. 85–156. Cambridge, UK: Academic Press.
- Raffa KF, Grégoire JC, Lindgren BS. 2015 Natural history and ecology of bark beetles. In *Bark beetles: biology and ecology of native and invasive species* (eds F Vega, RW Hofstetter), pp. 1–40. Cambridge, UK: Academic Press.
- Hofstetter RW, Affitto N, Bedoya CL, Yturralde K, Dunn DD. 2019 Vibrational behavior in bark beetles – applied aspects. In *Biotremology – studying vibrational behavior. Animal signals and communication series*, vol. 6 (ed. PSM Hill), pp. 415–435. London, UK: Springer
- Kirkendall LR 1983 The evolution of mating systems in bark and ambrosia beetles (Coleoptera: Scolytidae and Platypodidae). *Zool. J. Linn. Soc.* **77**, 293–352. (doi:10.1111/j.1096-3642.1983.tb00858.x)
- Wood S L. 1982 The bark and ambrosia beetles of North and Central America (Coleoptera: Scolytidae), a taxonomic monograph. *Great Basin Nat. Mem.* **6**, 1–1359.
- Grégoire JE, Raffa KF, Lindgren BF. 2015 Economics and politics of bark beetles. In *Bark beetles: biology and ecology of native and invasive species* (eds F Vega, RW Hofstetter), pp. 585–613. Cambridge, UK: Academic Press.
- Rudinsky JA, Michael RR. 1973 Sound production in Scolytidae: stridulation by female *Dendroctonus* beetles. *J. Insect. Physiol.* **19**, 689–705. (doi:10.1016/0022-1910(73)90078-4)
- Ryker LC, Rudinsky JA. 1976 Sound production in Scolytidae – acoustic signals of male and female *Dendroctonus valens* Leconte. *J. Appl. Entomol.* **80**, 113–118. (doi:10.1111/j.1439-0418.1976.tb03308.x)
- Barr BA. 1969 Sound production in Scolytidae (Coleoptera) with emphasis on the genus *Ips*. *Can. Entomol.* **101**, 636–672. (doi:10.4039/Ent101636-6)
- Lyal CHC, King T. 1996 Elytro-tergal stridulation in weevils (Insecta: Coleoptera: Curculionoidea). *J. Nat. Hist.* **30**, 703–773. (doi:10.1080/00222939600770391)
- Fleming AJ, Lindeman AA, Carroll AL, Yack JE. 2013 Acoustics of the mountain pine beetle (*Dendroctonus ponderosae*) (Curculionidae, Scolytinae): sonic, ultrasonic, and vibration characteristics. *Can. J. Zool.* **91**, 235–244. (doi:10.1139/cjz-2012-0239)
- Yturralde KM, Hofstetter RW. 2015 Characterization of stridulatory structures and sounds of the larger Mexican pine beetle, *Dendroctonus approximatus* (Coleoptera: Curculionidae: Scolytinae). *Fla. Entomol.* **98**, 516–527. (doi:10.1653/024.098.0219)
- Bedoya CL, Brockerhoff EG, Hayes M, Pawson SM, Najar-Rodriguez A, Nelson XJ. 2019 Acoustic communication of the red-haired bark beetle (*Hylurgus ligniperda*). *Physiol. Entomol.* **44**, 252–265. (doi:10.1111/phen.12301)
- Chesmore D, Schofield J. 2010 Acoustic detection of regulated pests in hardwood material. *EPPD Bulletin*. **40**, 46–51. (doi:10.1111/j.1365-2338.2009.02353.x)
- Mankin RW, Hagstrum DW, Smith MT, Roda AL, Kairo MTK. 2011 Perspective and promise: a century of insect acoustic detection and monitoring. *Am. Entomol.* **57**, 30–44. (doi:10.1093/ae/57.1.30)
- Jalinas JB, Güerri-Agulló B, Dosunmu OG, Haseeb M, Lopez-Llorca LV, Mankin RW. 2019 Acoustic signal applications in detection and management of *Rhynchophorus* spp. in fruit-crops and ornamental palms. *Fla. Entomol.* **102**, 475–479. (doi:10.1653/024.102.0303)
- Sutin A, Yakubovskiy S, Salloum HR, Flynn TJ, Sedunov N, Nadel H. 2019 Towards an automated acoustic detection algorithm for wood-boring beetle larvae (Coleoptera: Cerambycidae and Buprestidae). *J. Econ. Entomol.* **112**, 1327–1336. (doi:10.1093/jee/toz016)
- Burns SH. 1979 The absorption of sound by pine trees. *J. Acoust. Soc. Am.* **65**, 658–661. (doi:10.1121/1.382475)
- Price MA, Attenborough K, Heap NW. 1988 Sound attenuation through trees: measurements and models. *J. Acoust. Soc. Am.* **84**, 1836–1844. (doi:10.1121/1.397150)
- Li M, Van Renterghem T, Kang J, Verheyen K, Botteldooren D. 2020 Sound absorption by tree bark. *Appl. Acoust.* **165**, 107328. (doi:10.1016/j.apacoust.2020.107328)

29. Wassilieff C. 1996 Sound absorption of wood-based materials. *Appl. Acoust.* **48**, 339–356. (doi:10.1016/0003-682X(96)00013-8)
30. Legg M, Bradley S. 2016 Measurement of stiffness of standing trees and felled logs using acoustics: a review. *J. Acoust. Soc. Am.* **139**, 588–604. (doi:10.1121/1.4940210)
31. Brockerhoff EG, Knížek M, Bain J. 2003 Checklist of indigenous and adventive bark and ambrosia beetles (Curculionidae: Scolytinae and Platypodinae) of New Zealand and interceptions of exotic species (1952–2000). *N. Z. Entomol.* **26**, 29–44. (doi:10.1080/00779962.2003.9722106)
32. Le PN, Ambikairajah E, Epps J, Sethu V, Choi EHC. 2011 Investigation of spectral centroid features for cognitive load classification. *Speech Commun.* **53**, 540–551. (doi:10.1016/j.specom.2011.01.005)
33. Wanniarachchi WAM, Ranjith PG, Perera MSA, Rathnaweera TD, Lyu Q, Mahanta B. 2017 Assessment of dynamic material properties of intact rocks using seismic wave attenuation: an experimental study. *R. Soc. Open Sci.* **4**, 170896. (doi:10.1098/rsos.170896)
34. Yang H, Yu L, Wang L. 2015 Effect of moisture content on the ultrasonic acoustic properties of wood. *J. For. Res.* **26**, 753–757. (doi:10.1007/s11676-015-0079-z)
35. Wang X, Carter P, Ross RJ. 2007 Acoustic evaluation of wood quality in standing trees. Part 1: acoustic wave behaviour. *Wood Fiber Sci.* **39**, 28–38.
36. Grabianowski M, Manley B, Walker JCF. 2006 Acoustic measurements on standing trees, logs and green lumber. *Wood Sci. Technol.* **40**, 205–216. (doi:10.1007/s00226-005-0038-5)
37. Toulmin MJ, Raymond CA. 2007 Developing a sampling strategy for measuring acoustic velocity in standing *Pinus radiata* using the treetap time of flight tool. *N. Z. J. For. Sci.* **37**, 96–111.
38. Rudinsky JA, Michael RR. 1972 Sound production in Scolytidae: chemostimulus of sonic signal by the Douglas-fir beetle. *Science* **175**, 1386–1390. (doi:10.1126/science.175.4028.1386)
39. Bedoya CL, Nelson XJ, Hayes M, Hofstetter RW, Atkinson TH, Brockerhoff EG. 2019 First report of luminous stimuli eliciting sound production in weevils. *Sci. Nat.* **106**, 1–4. (doi:10.1007/s00114-019-1619-8)
40. McCarthy JK, Brockerhoff EG, Didham RK. 2013 An experimental test of insect-mediated colonisation of damaged *Pinus radiata* trees by sapstain fungi. *PLoS ONE* **8**, e55692. (doi:10.1371/journal.pone.0055692)
41. Bedoya CL. 2022 Code for: carolbedoya/beetle-sounds-inside-wood: version 1.0 (beetle_sounds_algorithms_v1.0). *Zenodo*. (doi:10.5281/zenodo.6757369)
42. Bedoya CL, Nelson XJ, Brockerhoff EG, Pawson S, Hayes M. 2022 Experimental Characterization and Automatic Identification of Stridulatory Sounds Inside Wood - Supplementary Information (Data). Figshare. (doi:10.6084/m9.figshare.19233087.v2)